# TRANSFUSION

# Antibody profiles in COVID-19 convalescent plasma prepared with amotosalen/UVA pathogen reduction treatment

Anil Bagri[1] | Rafael R. de Assis[2] | Cheng-Ting Tsai[3] | Graham Simmons[4] |
Zhen W. Mei[5] | Melissa Von Goetz[1] | Michelle Gatmaitan[1] | Mars Stone[4] |
Clara Di Germanio[4] | Rachel Martinelli[4] | Orsolya Darst[4] |
Jowin Rioveros[5] | Peter V. Robinson[3] | Dawn Ward[5] | Alyssa Ziman[5] |
David Seftel[3] | Saahir Khan[6] | Michael P. Busch[4] | Philip L. Felgner[2] |
Laurence M. Corash[1]

[1]Transfusion Medicine Research, Cerus Corporation, Concord, California, USA

[2]Department of Physiology and Biophysics, School of Medicine, University of California Irvine, Irvine, California, USA

[3]Enable Biosciences Inc, South San Francisco, California, USA

[4]Scientific Research Programs, Vitalant Research Institute, San Francisco, California, USA

[5]Wing-Kwai and Alice Lee-Tsing Chung Transfusion Service, Department of Pathology and Laboratory Medicine, David Geffen School of Medicine at University of California, Los Angeles, California, USA

[6]Division of Infectious Diseases, Department of Medicine, University of California Irvine Health, Orange, California, USA

**Correspondence**
Laurence M. Corash, 1220 Concord Ave, Concord, CA 94520, USA.
Email: lcorash@cerus.com

**Abstract**

**Background:** COVID-19 convalescent plasma (CCP), from donors recovered from severe acute respiratory syndrome coronavirus-2 (SARS-CoV-2) infection, is one of the limited therapeutic options currently available for the treatment of critically ill patients with COVID-19. There is growing evidence that CCP may reduce viral loads and disease severity; and reduce mortality. However, concerns about the risk of transfusion-transmitted infections (TTI) and other complications associated with transfusion of plasma, remain. Amotosalen/UVA pathogen reduction treatment (A/UVA-PRT) of plasma offers a mitigation of TTI risk, and when combined with pooling has the potential to increase the diversity of the polyclonal SARS-CoV-2 neutralizing antibodies.

**Study design and methods:** This study assessed the impact of A/UVA-PRT on SARS-CoV-2 antibodies in 42 CCP using multiple complimentary assays including antigen binding, neutralizing, and epitope microarrays. Other mediators of CCP efficacy were also assessed.

**Results:** A/UVA-PRT did not negatively impact antibodies to SARS-CoV-2 and other viral epitopes, had no impact on neutralizing activity or other

potential mediators of CCP efficacy. Finally, immune cross-reactivity with other coronavirus antigens was observed raising the potential for neutralizing activity against other emergent coronaviruses.

**Conclusion:** The findings of this study support the selection of effective CCP combined with the use of A/UVA-PRT in the production of CCP for patients with COVID-19.

**KEYWORDS**
FFP transfusion, plasma derivatives, transfusion-transmitted disease—other

# 1 | INTRODUCTION

In December 2019, a novel, highly contagious coronavirus, severe acute respiratory syndrome coronavirus-2 (SARS-CoV-2) identified in Wuhan, China, was determined to be the causative agent of the coronavirus disease, COVID-19. It has rapidly spread around the world and was declared a pandemic by the World Health Organization.[1,2] Patients infected with SARS-CoV-2 have presentations ranging from asymptomatic to severe pneumonia, multi-organ failure, and death. As of February 15, 2021, 110 million individuals have been infected worldwide with over 2.4 million deaths.

Therapeutic options for the treatment of COVID-19 are limited and primarily supportive.[3] One readily available therapeutic option is convalescent plasma (CP) with neutralizing antibodies (Nabs) from recovered COVID-19 donors. CP has been used to treat other viral diseases including: severe acute respiratory syndrome (SARS), Middle East Respiratory Syndrome (MERS), Ebola, Influenza A (H1N1), and Argentine Hemorrhagic Fever.[4–10]

Although not confirmed by randomized controlled trials (RCTs), there is evidence that effective CP from COVID-19 patients (CCP) may reduce disease severity and reduce mortality.[11–13] CCP may be superior to other passive immunotherapies such as hyperimmune globulin preparations or recombinant antibodies because it has the potential to reverse COVID-19 coagulopathy and endothelial cell injury that contribute to morbidity.[14–19]

There is uncertainty regarding the safety and efficacy of CCP. Lack of adequately powered RCTs and inconsistent characterization of antibody profiles, including Nab levels, has made it challenging to arrive at definitive conclusions about CCP efficacy. In addition, concerns persist about the risk of TTI. Pathogen reduction treatment (PRT) of plasma offers mitigation of TTI risk[20] and enables pooling which decreases component variability and increases antibody diversity, theoretically conferring greater activity against pathogens with high mutation rates such as SARS-CoV-2.[21] However, the impact of PRT on CCP is poorly understood. The present study presents a detailed characterization of the impact of amotosalen/UVA PRT on CCP antibody profiles using a variety of complementary methodologies. The impact of PRT on other potential biologic mediators of CCP efficacy also was assessed.

# 2 | METHODS

## 2.1 | PRT and collection of pre-PRT and post-PRT samples

Apheresis CCP was collected by the *Trima Accel* Collection System (Terumo BCT, Lakewood, CA) following verification of prior SARS-CoV-2 infection. The collection procedures followed routine blood donor collection processes per AABB regulations and UCLA Blood & Platelet Center standard operating procedures. This study was approved by the institutional review board at UCLA (#20-001619) as a no-subject contact study with a waiver of consent.

PRT was performed using the INTERCEPT Blood System for Platelets and Dual Storage (DS) Platelet Processing kits (Cerus Corporation, Concord). A 3 ml baseline plasma sample was taken prior to PRT. After illumination (3 J/cm$^2$), CCP was transferred to the Compound Adsorption Device before transfer to storage containers. Prior to freezing ($\leq-18°C$), a 3 ml post-PRT sample was collected.

## 2.2 | Antibody dependent agglutination PCR, COVAM antigen microarray, reporter viral particle neutralization, and cytokine profiling analysis of CCP samples

Detection of CCP Ab against spike (S) protein, nucleocapsid (N) protein, and neutralizing antibody (Nab) to S binding to the soluble ACE-2 receptor was performed by using PCR-based methods (Appendix S1).[22–24] The basis

of the neutralization assay is through the use of complimentary small DNA sequence (bar codes) attached to the S1 RBD antigen and to the ACE-2 receptor. In the presence of antibody to S1 RBD antigen, binding to the ACE-2 receptor is neutralized, and the DNA bar codes cannot be ligated and amplified. The Nab titer is correlated with the level of inhibition ($\Delta$Ct) based on positive and negative control samples. In the absence of Nab, S1 RBD antigen binds to the ACE-2 receptor, the complimentary DNA bar codes are ligated and amplified indicating the absence of Nab with short $\Delta$Ct.

The coronavirus antigen microarray (COVAM) analysis including mean fluorescence intensity (MFI) normalization, unsupervised cluster analysis, and principal component analysis were performed as previously described (Appendix S1).[25]

Neutralizing activity with the SARS-CoV-2 reporter viral particle neutralization (RVPN) assay was as previously described (Appendix S1).[26]

Cytokine profiling of CCP was performed at Myriad RBM (Austin, TX) with a custom multiplexed Luminex assay (Appendix S1).

## 2.3 | Statistical analysis

Assay specific statistical analyses were performed as described in Appendix S1. Comparison of Pre-PRT and Post-PRT samples was performed by Wilcoxon matched pairs signed rank test, best fit curves and $R^2$ (correlations) were assessed based on linear trendlines unless otherwise specified. Error bars represent SEM. Unless otherwise specified, statistical analysis was performed in Microsoft Office 365 Excel (Microsoft, Seattle, WA) or GraphPad Prizm 7 (GraphPad Software, San Diego, CA).

## 3 | RESULTS

### 3.1 | Impact of amotosalen/UVA pathogen reduction treatment on antibody binding to SARS-CoV-2N and S1 proteins

Total immunoglobulin (Ig) concentration was quantified from 42 CCP donors prior to and after PRT. There was no difference between Pre-PRT and Post-PRT total Ig levels ($p = .36$). The Post-PRT/Pre-PRT ratio was 1.01 (SEM 0.02) indicating that overall, immunoglobulins were not impacted by PRT.

To determine the impact of A/UVA-PRT on SARS-CoV-2 antibodies, CCP were assayed using a sensitive and specific Antibody dependent agglutination PCR (ADAP) PCR based assay to quantify antibody binding to

N and S1 proteins.[23] Antibody activity was measured by the change in cycle time ($\Delta$Ct) compared to a negative control plasma. For N and S1 ADAP assays, 37 of 42 plasmas (88%) had activity, and 5 were negative. Excluding the negative samples, no correlation for reactivity ($R^2 = 0.24$) between N- and S1-$\Delta$Ct values was identified. There was a broad distribution of $\Delta$-Ct values for both antibodies post PRT (Figure 1A,B). Antibody responses to S1 were higher than to N suggesting that S1 is a more potent immunogen. The Post-PRT/Pre-PRT ratio was 1.01 (SEM 0.01) for Ab to N and 0.99 (SEM 0.01) for Ab to S1 indicating the negligible impact of PRT (Figure 1C). An assessment by donor confirmed that most CCP had less than 10% change from baseline after PRT (Figure 1D). There was no correlation in the magnitude or direction of the $\Delta$Ct ratio for N protein with the $\Delta$Ct ratio for S1 protein (Figure 1D). To determine if samples with lower levels of antibody were particularly susceptible to PRT, the $\Delta$Ct ratio was evaluated as a function of $\Delta$Ct level. No correlation was identified (Figure 1E,F) indicating that A/UVA-PRT treatment did not affect antibodies in a concentration dependent manner.

### 3.2 | Impact of amotosalen/UVA pathogen inactivation on IgG, IgM, and IgA antibodies to multiple SARS-CoV-2 antigens

The impact of A/UVA-PRT on antibodies that bind to a broad range of SARS-CoV-2 epitopes, including different subregions of the spike protein, was evaluated using the COVAM assay with 11 purified recombinant antigens on nitrocellulose-coated slides.[27] The microarray also contains other coronavirus antigens implicated in SARS-CoV-1, MERS-CoV, 12 other seasonal coronaviruses, and other respiratory viruses including: influenza, adenovirus, and RSV that may result in concurrent respiratory disease.[25]

The heatmap of antigen binding in the COVAM microarray (Figure 2A) shows heterogeneous IgG reactivity to SARS-CoV-2 and other viral antigens. Limited IgM binding was detected for SARS-CoV-2 antigens consistent with the delayed timeframe of plasma collection with respect to onset of symptoms (average of $55 \pm 22$ days from symptom onset; Data not shown). Principal component analysis[25] of IgG immunoreactivity to SARS-CoV-2 was used to classify the CCP into four distinct populations (Figure 2B). These were categorized as non-reactive (Group 1–9/42, 21%); broadly reactive (Group 2–11/42, 26%); variably reactive with more reactivity to N protein and lower reactivity to other antigens (Group 3–6/42, 14%); and variably reactive with more reactivity to S1
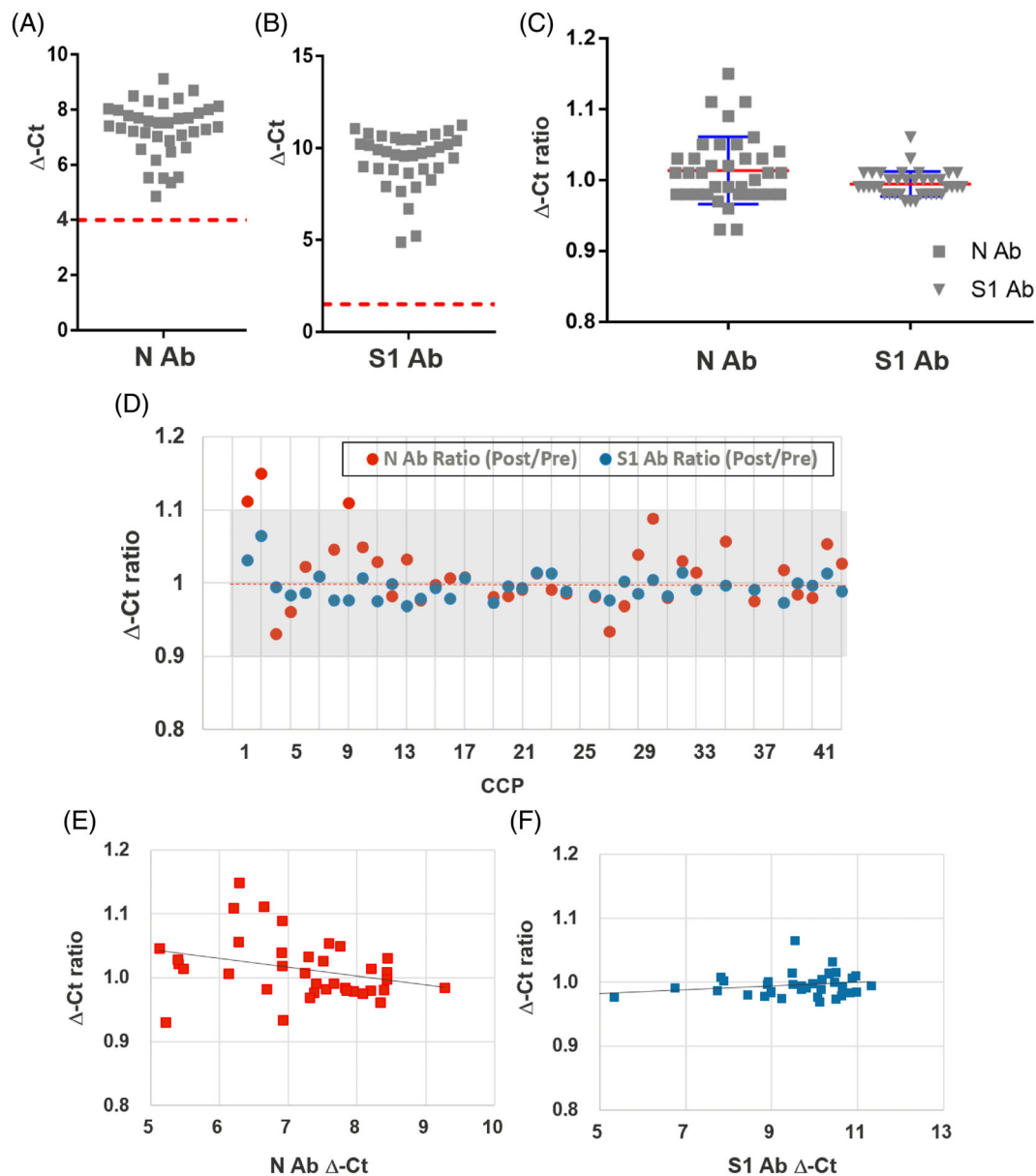
**FIGURE 1** Amotosalen/UVA light pathogen inactivation treatment (PRT) does not impact SARS-CoV-2 antibody binding using the highly sensitive ADAP assay. (A) Distribution of Δ-Ct measurements for antibodies binding to the nucleocapsid (N) protein. The cut-off of positivity is depicted with the dashed red line. (B) Distribution of Δ-Ct measurements for antibodies binding to the Spike 1 (S1) protein. The cut-off of positivity is depicted with the dashed red line. (C) The distribution, average (red line) and SEM (blue error bars) of ratio of antibody Post-PRT to Pre-PRT Δ-Ct (Δ-Ct ratio) for the N and the S1 proteins. (D) Δ-Ct ratio for individual COVID-19 convalescent plasma antibodies for N (red) and the S1 (blue) ADAP assay. Ideal ratio of 1 is highlighted with a dotted red line, and the 10% change is delineated by gray shading. (E) Δ-Ct ratio for the N protein antibody as a function of N protein Δ-Ct. The linear trend line depicts that the ratios have a minimal change over the dynamic range of the assay. (F) Δ-Ct ratio for the antibody to Spike (S1) protein as a function of antibody level to S1 protein Δ-Ct. The linear trend line depicts that the ratios have a minimal change over the dynamic range of the assay. ADAP, Antibody dependent agglutination PCR; PRT, pathogen reduction treatment; SARS-CoV-2, severe acute respiratory syndrome coronavirus-2 [Color figure can be viewed at wileyonlinelibrary.com]

protein and lower reactivity to N protein (Group 4–16/42, 38%). When CCP are clustered into these 4 groups, the heat map defined these distinct immunoreactivity profiles (Figure S1A). CCP negative for Ab to S1 and N by ADAP assay, described above, co-located to the non-reactive COVAM Group 1.

The heatmap of immunoreactivity (Figure 2A) showed that compared to Pre-PRT, the adjacent Post-PRT levels were largely unchanged. This was confirmed by the assessment of the Post-PRT/Pre-PRT ratio of mean fluorescent intensity (MFI). The average MFI ratio was 1.00 (SEM 0.01) for IgG, 0.97 for IgM (SEM 0.03), and

1.02 for IgA (SEM 0.03) (Figure 2C). Similar patterns also were noted for IgG, IgM, and IgA binding to other coronaviruses, influenza virus, and other common respiratory viruses. There was no correlation of the MFI Post-PRT/ Pre-PRT ratio with relative signal strength (Figure 2D). Overall, the Post-PRT/Pre-PRT MFI ratio was 1.01 (SEM 0.01) for IgG across all epitopes, 0.95 (SEM 0.02) for IgM and 0.98 (SEM 0.01) for IgA confirming that for specific
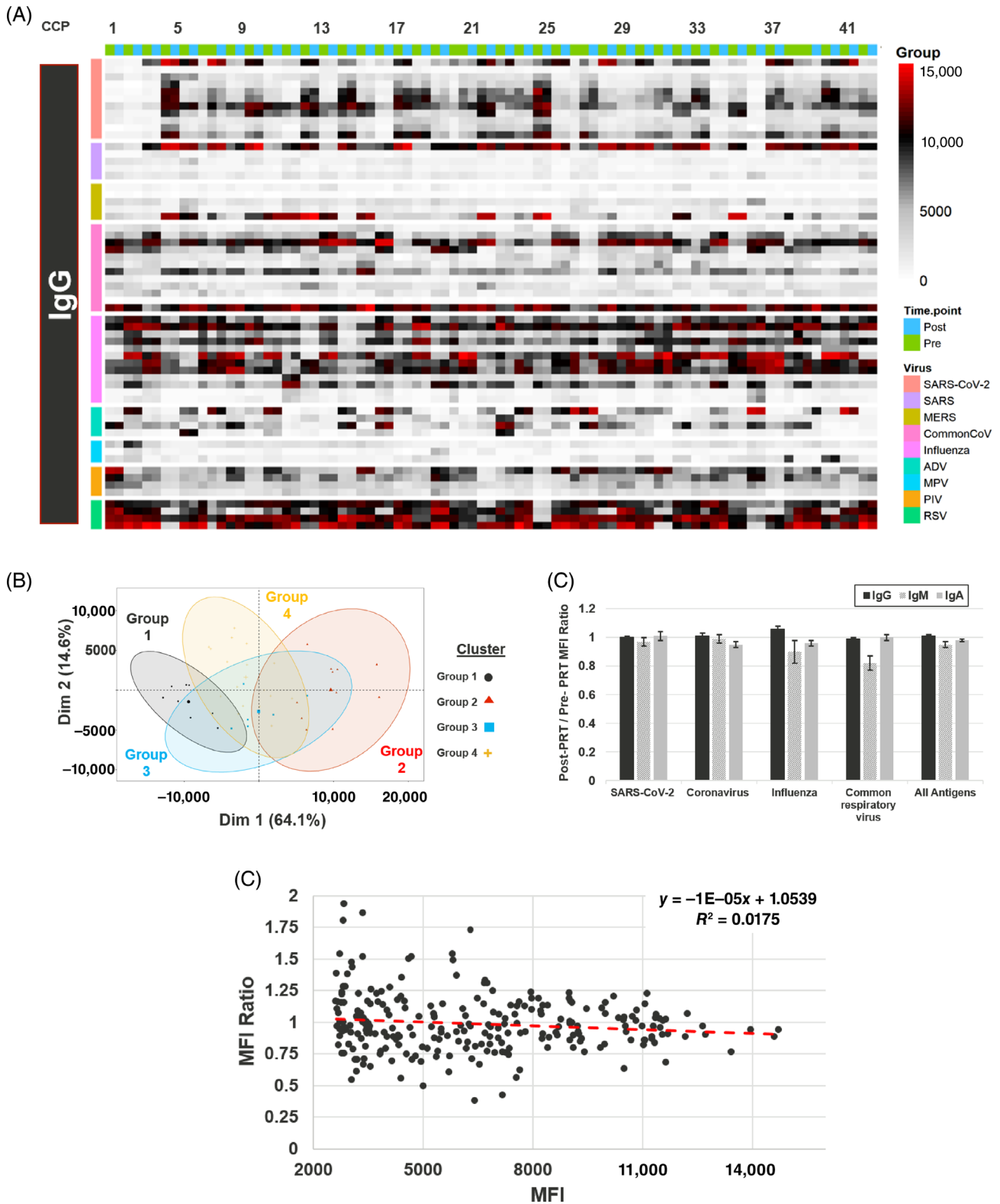


FIGURE 2    Legend on next page.

epitopes and globally, A/UVA-PRT did not impact immunoglobulin binding to a broad spectrum of viral antigens.

At present, CCP is largely provided as single plasma units. To define the overall impact of PRT on antibody binding, scatter plots comparing Pre-PRT, and Post-PRT MFI for IgG reactivity for all COVAM epitopes for each individual CCP were evaluated (Figures 3A and S1A). The correlation coefficients of IgG for the majority of CCP approach 1 (Figure 3B), indicating that IgG from most donors was minimally impacted by PRT. Similar trends were seen for IgM and IgA. Cluster analysis for post PRT plasma samples, excluding Group 1 without activity, yielded the same assignments as the pre-PRT samples (Figure 3C) consistent with a lack of PRT impact on antigen binding or classification.

## 3.3 | Impact of amotosalen/UVA pathogen inactivation treatment on SARS-CoV-2 neutralizing activity

Measurement of viral neutralization is a key metric to assess CCP potency. The standard for assessing neutralization is the virus plaque reduction neutralization assay (PRNT). To facilitate the evaluation of neutralization activity, we used a sensitive cell-free assay based on the interaction of recombinant SARS-CoV-2 Spike 1 protein containing the RBD with the ACE-2 receptor. This soluble ACE-2 Blocking Nab assay using the ADAP platform (Figure S2A), is sensitive and specific.[24] The activity was measured by the change in cycle time ($\Delta$Ct) compared to a negative control plasma. Of the 42 CCP assessed, 36 (86%) were positive and 6 were negative. Five of the 6 ACE-2 negative CCP localized to COVAM cluster Group 1 (non-reactive) with the sixth CCP localized to Group 3. There was a broad distribution of ACE-2 Blocking $\Delta$Ct (Figure 4A). The average Post-PRT/Pre-PRT ratio was 0.99 (SEM 0.05) indicating minimal impact of

A/UVA-PRT on CCP Nab activity (Figure 4B). The majority (>80%) of donors had less than 10% loss of Nab activity due to PRT (Figure 4C). The $\Delta$Ct ratio plotted as a function of ACE-2 Blocking $\Delta$Ct activity showed no correlation (Figure S2C).

A pseudovirus reporter viral neutralization (RVPN) assay using green fluorescent protein also was used to evaluate the impact of PRT on Nab activity (Figure S2B). This assay measures functional neutralizing activity with susceptible cells, and it has demonstrated comparability to PRNT assays.[28–30] A metric of neutralization capacity, $NT_{50}$ (defined as the dilution at which the luciferase activity was reduced by 50% compared with the untreated virus), was calculated for each sample. Of the 42 CCP, 36 (86%) were positive for neutralization and 6 were negative. Four of the 6 negative CCP were in COVAM cluster Group 1 with the fifth and sixth CCP localizing to groups 3 and 4 respectively. There was a broad distribution of RVPN $NT_{50}$ values (Figure 4D) consistent with the results of ACE-2 Blocking assay. The average Post-PRT/Pre-PRT ratio was 1.14 (SEM 0.08, Figure 4E). The majority (>80%) had less than 10% loss of Nab activity (Figure 4F); and the $NT_{50}$ ratio evaluated as a function of $NT_{50}$ signal strength identified no correlation (Figure S2D). A direct comparison of the two neutralization assays (Figure 4G) demonstrated high correlation ($R^2 = 0.722$) with a near-linear relationship (best-fit curve, $y = 28.3X^{1.08}$).

Nab levels also were compared to binding to selective epitopes from the COVAM microarray for IgG and IgA subclasses. Strong correlations were observed between ACE-2 Blocking and IgG binding to Spike 1 protein (SARS-CoV-2.S1.mFcTag—$R^2 = 0.700$) and S1.RBD (SARS-CoV-2.S1.RBD—$R^2 = 0.673$) (Figure S3A,B). Similar correlations were observed for RVPN $NT_{50}$ levels (Figure S3E,F). An assessment of correlations of IgA antibody binding to SARS-CoV-2 antigens in the COVAM microarray data with Nab activity did not identify relationships of similar strength (Figure S3C,D,G,H). Thus, most of the neutralizing activity appeared to be mediated by IgG.

**FIGURE 2** Amotosalen/UVA light pathogen reduction treatment (PRT) does not impact antibodies to a broad range of viral antigens. (A) Heatmap for viral antigen microarray. The heatmap shows mean fluorescence intensity across four replicates, for IgG against each antigen organized into rows color coded by viral class (right side), for sera organized into columns of paired Pre-PRT (green) and Post-PRT (blue) COVID-19 convalescent plasma (CCP) samples. (B) Principal component analysis showing the spatial distribution of the pre-PRT samples for all donors along the first and second principal components. Samples were grouped into four populations: non-reactive (G1—Black); broadly reactive (G2—Red); primarily N protein reactive (G3—Blue—samples that are highly reactive to N protein but lower reactive to the other antigens) and; Primarily spike reactive (G4—Yellow—samples that are reactive to spike but with low reactivity to N protein). (C) The average ratio of Post-PRT to Pre-PRT mean fluorescent intensity (MFI) (MFI ratio) for IgG, IgM and IgA binding to epitopes from SARS-CoV-2, severe acute respiratory syndrome coronavirus-2 (SARS-CoV-2), other coronaviruses, Influenza, other common respiratory viruses and all epitopes on the viral antigen microarray. Error bars represent SEM. (D) MFI ratio for IgG binding to SARS-CoV-2 epitopes on the viral antigen microarray as a function of signal strength (Normalized MFI). The linear trend line red dashed line demonstrates that the ratios have a minimal change over the dynamic range of the assays [Color figure can be viewed at wileyonlinelibrary.com]

(A)



(B)



(C)
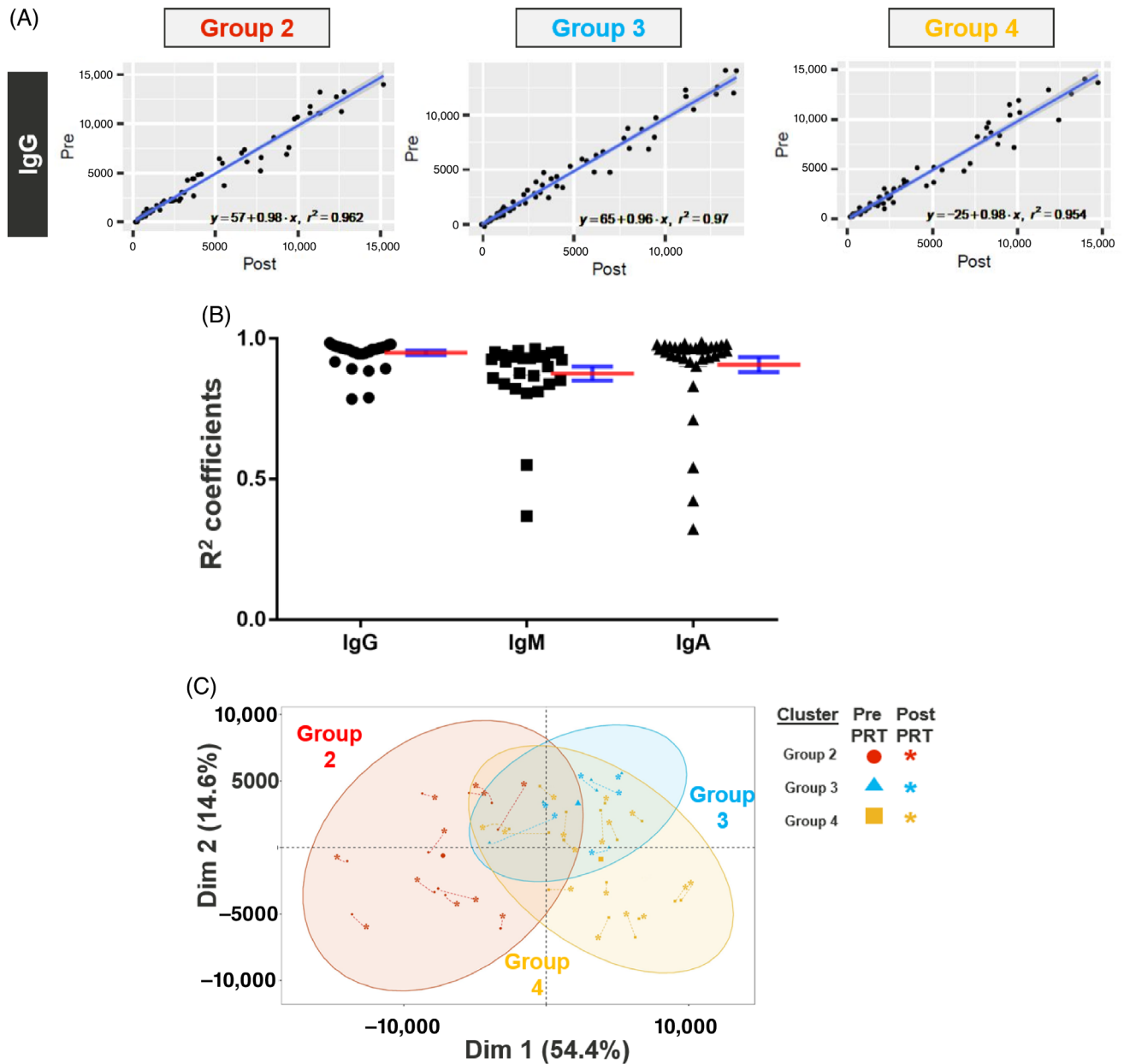


**FIGURE 3** Amotosalen/UVA light PRT does not broadly impact antibodies in a given CCP sample. (A) Scatter plots of all IgG Pre-PRT to Post-PRT normalized MFI data above the threshold of positivity for a given CCP for a representative donor from Group 2, 3 and 4. Best fit line is shown in blue with the 95% CI highlighted in dark gray. (B) Scatter plot of $R^2$ values for IgG, IgM and IgA for each individual CCP with mean and SEM delineated. (C) Principal component analysis depicting that PRT does not impact CCP cluster designation for Group 2, 3 or 4. CCP, COVID-19 convalescent plasma; MFI, mean fluorescent intensity; PRT, pathogen reduction treatment [Color figure can be viewed at wileyonlinelibrary.com]

## 3.4 | Levels of fibrinogen and pro-inflammatory cytokines in amotosalen/UVA pathogen inactivated CCP

Other studies have identified coagulopathy in patients with severe COVID-19.[14–16,18] Furthermore, endothelial cell damage in COVID-19 is postulated to result in altered blood vessel barrier integrity leading to end-organ damage, a pro-coagulative state, and vascular and parenchymal inflammation.[17,19] Fibrinogen has been hypothesized to provide an endothelial protective function.[31] Therefore, it was relevant to understand the impact of A/UVA-PRT on fibrinogen levels. We observed a minimal impact of A/UVA PRT on fibrinogen levels (Figure 5A). Vascular endothelial growth factor (VEGF) is also known to protect damaged endothelial cells. VEGF levels were characterized in the CCP samples. Of the 42 CCP, 12 (29%) had quantifiable levels of VEGF (>1 ng/ml) with an average of 93.4 ng/ml
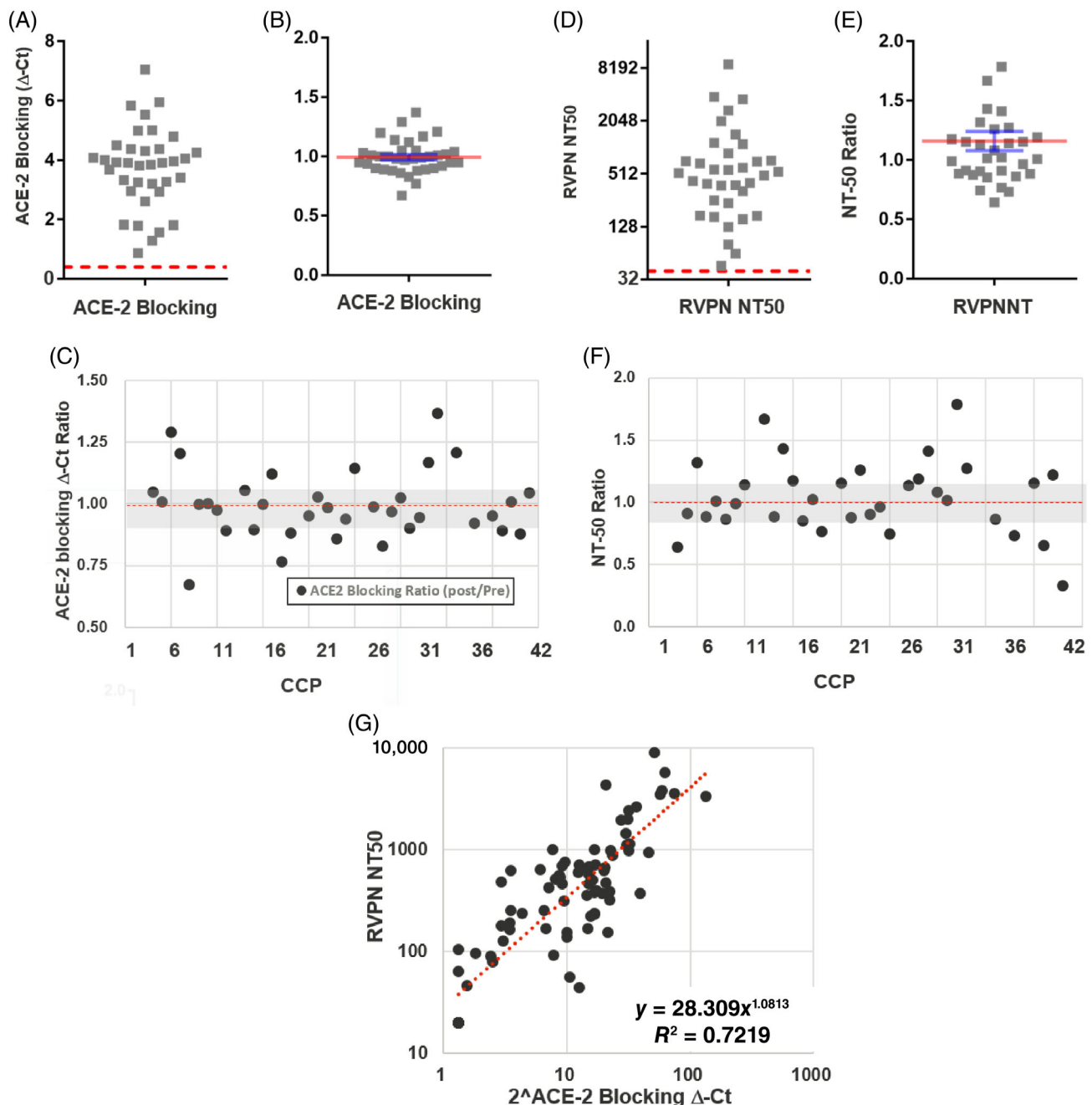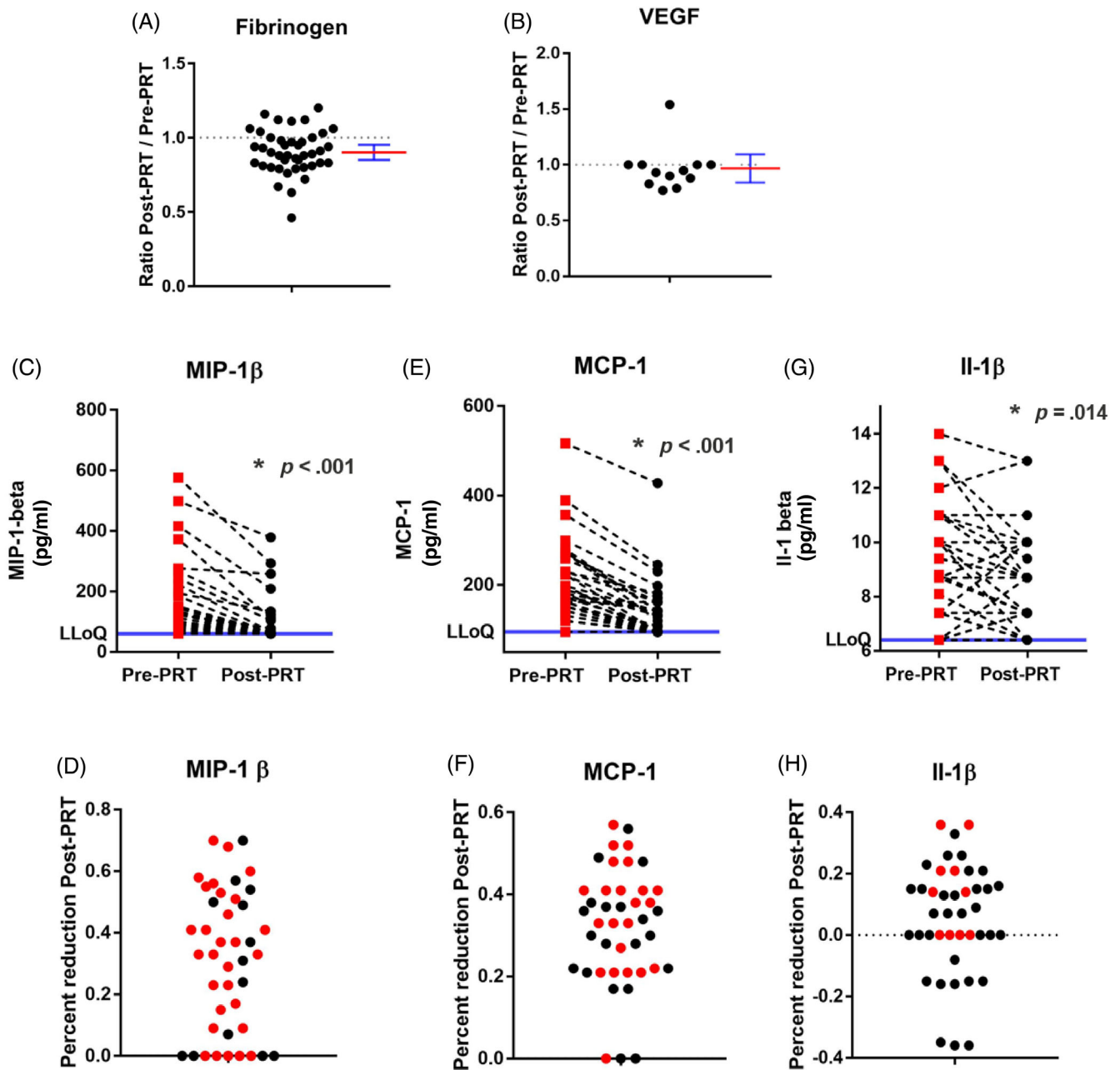
**FIGURE 4** Amotosalen/UVA light pathogen inactivation treatment (PRT) does not impact SARS-CoV-2 neutralizing activity. (A) Distribution of ACE-2 Blocking $\Delta$-Ct. The assay cut-off of positivity is depicted with the dashed red line. (B) The distribution, average (red line) and SEM (blue error bars) of ratio of Post-PRT to Pre-PRT ACE-2 Blocking $\Delta$-Ct. (C) ACE-2 blocking $\Delta$-Ct Ratio for individual CCP for ACE-2 blocking ADAP assay. Ideal ratio of 1 is highlighted with a dotted red line, and the 10% change is delineated by gray shading. (D) Distribution of RVPN NT50. The assay cut-off of positivity is depicted with the dashed red line. (E) The distribution, average (red line) and SEM (blue error bars) of ratio of Post-PRT to Pre-PRT RVPN NT50. (F) Ratio of Post-PRT to Pre-PRT NT50 (NT50 ratio) values for individual donors in the RVPN neutralization assay. Ideal ratio of 1 is highlighted with a dotted red line, and the 10% change is delineated by gray shading. (G) Scatter plot depicting correlation of RVPN NT50 with ACE-2 Blocking $\Delta$-Ct. ADAP, Antibody dependent agglutination PCR; CCP, COVID-19 convalescent plasma; PRT, pathogen reduction treatment; SARS-CoV-2, severe acute respiratory syndrome coronavirus-2 [Color figure can be viewed at wileyonlinelibrary.com]

(SEM 2.2 ng/ml). PRT treatment did not impact VEGF levels ($p = .33$ by paired $t$-test), with the average Post-PRT/Pre-PRT ratio of 0.97 (SEM 0.06, Figure 5B).

There is evidence that severely ill COVID-19 patients have high levels of pro-inflammatory cytokines.[32] In these patients, Cytokine Storm Syndrome (CSS) may be a major

**FIGURE 5** Amotosalen/UVA light pathogen inactivation treatment (PRT) treatment impacts pro-inflammatory cytokines but does not impact vascular protective factors. (A) The distribution, average (red line) and SEM (blue error bars) of ratio of Post-PRT to Pre-PRT Fibrinogen levels. (B) The distribution, average (red line) and SEM (blue error bars) of ratio of Post-PRT to Pre-PRT VEGF levels. (C) Graph of MIP-1β (pg/ml) for paired Pre-PRT (red squares) and Post-PRT (black circles) samples. The LLoQ for MIP-1β assay is delineated as a blue line ($p < .001$). (D) Scatter plot of the percent reduction of MIP-1β levels Post-PRT compared to Pre-PRT. Donors for which levels were reduced to LLoQ are highlighted in red. (E) Graph of MCP-1 (pg/ml) for paired Pre-PRT (red squares) and Post-PRT (black circles) samples. The LLoQ for MCP-1 assay is delineated as a blue line ($p < .001$). (F) Scatter plot of the percent reduction of MCP-1 levels Post-PRT compared to Pre-PRT. Donors for which levels were reduced to LLoQ are highlighted in red. (G) Graph of Interleukin-1 (Il-1)β (pg/ml) for paired Pre-PRT (red squares) and Post-PRT (black circles) samples. The LLoQ for Il-1β assay is delineated as a blue line ($p = .014$). (H) Scatter plot of the percent reduction of Il-1β levels Post-PRT compared to Pre-PRT. Donors for which levels were reduced to LLoQ are highlighted in red. PRT, pathogen reduction treatment; VEGF, vascular endothelial growth factor [Color figure can be viewed at wileyonlinelibrary.com]

driver of acute respiratory distress syndrome (ARDS) and end-organ damage.[33,34] We measured the level of cytokines in CCP and the impact of A/UVA-PRT, we compared Pre-PRT and Post-PRT levels using a highly sensitive and

specific Luminex-based multiplexed cytokine panel. Many cytokines were largely absent (below the lower level of quantification) from both Pre-PRT and Post-PRT CCP including: GM-CSF, TNF alpha, Interleukin (IL)-2, IL-3,

FIGURE 6    Cross-reactivity between SARS-CoV-2 and related coronaviruses suggests the potential for CCP to provide protection against other coronaviruses. (A) Correlation between SARS-CoV-2 and SARS-CoV Nuclear protein reactivity in the viral antigen microarray. Logarithmic trendline with $R^2$ value of 0.71 is depicted with a dashed line. (B) Heatmap of COVAM MFI for SARS-CoV-2 Spike protein (middle column) and MERS-CoV-1 Spike protein (left column) reactivity of CCP re-organized into the 4 COVAM reactivity clusters (right column: group 1—black; group 2—red; group 3—blue; group 4—yellow). (C) Correlation between SARS-CoV-2 and MERS-CoV Spike protein reactivity in the viral antigen microarray. A population of donors with high SARS-CoV-2 and MERS-CoV reactivity and highlighted in the red dashed oval. (D) Correlation of ACE-2 Blocking in the ADAP assay with MERS-CoV spike protein reactivity in the viral antigen microarray for the subpopulation of donors with high SARS-CoV-2 and MERS-CoV Spike protein reactivity highlighted in (B). Linear trend line with R-squared value of 0.84 shown. The cut-off for positive ACE-2 blocking ADAP assay is also depicted. ADAP, Antibody dependent agglutination PCR; CCP, COVID-19 convalescent plasma; COVAM, coronavirus antigen microarray; MERS, Middle East Respiratory Syndrome; MFI, mean fluorescent intensity; PRT, pathogen reduction treatment; SARS-CoV-2, severe acute respiratory syndrome coronavirus-2 [Color figure can be viewed at wileyonlinelibrary.com]
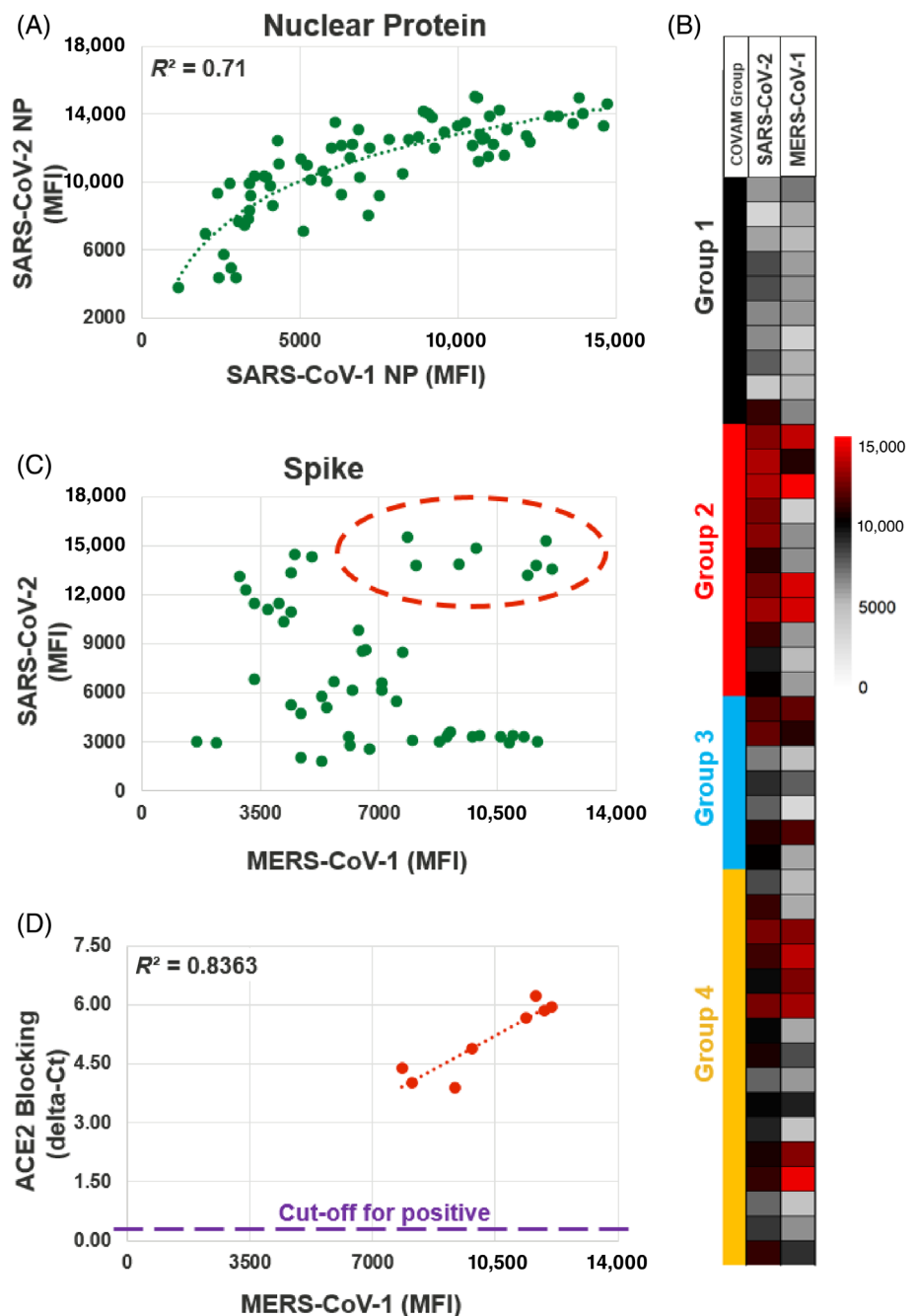


IL-4, IL-5, IL-6, IL-7, IL-10, and IL-17. Notably, several cytokines implicated in CSS were detected in Pre-PRT CCP, including IL-1 β (9.66 [SEM 0.30] pg/ml), MCP-1 (203.88 [SEM 12.81] pg/ml), and MIP-1β (169.73 [SEM 22.28] pg/ml) at levels higher than reported in normal subject plasma: IL-1β at 0.5 pg/ml,[35] MCP-1 at 69-174 pg/ml,[36] and MIP-1β at 17-41 pg/ml.[37] Unexpectedly, PRT reduced the levels of all three of these pro-inflammatory cytokines (MIP-1β $p < .001$, MCP-1 $p < .001$, and IL-1β $p = .014$). MIP-1β and MCP-1 were more reduced with the levels in a majority of CCP reduced to the lower level of quantification (Figure 5C–F). The impact of PRT on IL-1β was more heterogeneous. Finally, anti-inflammatory cytokines including Interleukin-1 receptor antagonist (IL-1ra) also were assessed. We found these to be unchanged in Post-PRT samples when compared to Pre-PRT samples ($p = .17$) with a Post-PRT/Pre-PRT ratio of 0.99 (SEM 0.06).

## 3.5 | Identification of CCP with cross-reactive antibodies to other coronaviruses

To evaluate the potential cross reactivity of COVID-19 CCP with other coronaviruses, an analysis was performed with the COVAM microarray, which contained shared epitopes for SARS-CoV-1 and MERS-CoV viruses. There

was a strong correlation between SARS-CoV-2 and SARS-CoV-1N protein reactivity ($R^2 = 0.71$—Figure 6A) consistent with the high amino acid (aa) identity reported.[38] Surprisingly, given the high homology for spike protein between SARS-CoV-1 and SARS-CoV-2, little cross-reactivity was observed. Similarly, for MERS-CoV, there was little cross-reactivity observed for N protein (data not shown). However, by COVAM there was significant cross-reactivity observed for MERS spike protein (Figure 6D). This finding was unexpected given the even lower aa identity between SARS-CoV-2 and MERS-CoV-1 spike protein. While there was poor overall correlation between the MFI for these two epitopes, a small proportion of CCP exhibited high SARS-CoV-2 and MERS-CoV spike immunoreactivity (4 of 42 CCP—10%; Figure 6B). These CCP exhibited high levels of Nab activity by the ACE-2 Blocking (Figure 6C) and RVPN assays. Notably, these CCP with high SARS-CoV-2 spike protein reactivity comprised 36% of the COVAM Group 2 cluster (Figure 3B).

# 4 | DISCUSSION

## 4.1 | Impact of A/UVA pathogen reduction on antibodies to SARS-CoV-2

Transfusion of CCP has shown potential benefit to patients with acute COVID-19. PRT of CCP is relevant to reduce the risk of TTI because CCP donors may transmit unrecognized pathogens and CCP recipients may be immune suppressed and at increased risk for TTI. Furthermore, PRT may facilitate the pooling of CCP from different donors to optimize antibody diversity while mitigating TTI risk of multiple donor exposures. Previous studies have generally reported that ~90% of donors with SARS-CoV-2 infection produce SARS-CoV-2 reactive antibodies.[39–41] The present study reports a similar positive rate ranging from 79% to 88% of CCP components. We utilized multiple assays to characterize antibodies in CCP for SARS-CoV-2 epitope reactivity and neutralization capacity. CCP from 42 recovered donors displayed a broad range of antibody profiles.

Cumulatively, our data conclusively demonstrate that A/UVA-PRT does not negatively impact immunoglobulin levels or neutralizing activity measured by two different assays. Although most of the analyses supporting these conclusions were performed on Abs binding to SARS-CoV-2 antigens, the analysis of antibodies to a broad array of viral antigens of other respiratory viruses confirmed and extended previous observations with Ebola convalescent plasma[42] confirming that A/UVA PRT does not impair antibody reactivity. This suggests that the findings apply broadly to Ig in convalescent plasma which is important as

there are several potentially pandemic viruses[43–44] for which convalescent plasma may be beneficial.

In our study, CCP demonstrated a broad range of antibody reactivity for most epitopes. We utilized this broad range to evaluate the impact of antibody concentration on PRT effects on epitope binding and neutralization. For the large part, the trend lines for these analyses demonstrates that ratios have minimal change over the dynamic range of the assays. The slight downward trend at higher values observed for some analytes may suggest that any impact is more readily observable at higher levels of antibody, but this minimal impact is unlikely to affect overall CCP activity at these higher antibody levels. To mitigate against potential assay artifacts, we employed multiple approaches to elucidate the impact of A/UVA-PRT on CCP antibodies. The consistency of observations between assay methods reinforces the study conclusions. CCP negative for antibody to N and S1 antigens by the ADAP assay were also classified as nonreactive (group 1) in the COVAM microarray analysis; and were largely negative for RVPN and ACE-2 blocking activity. Thus, any of these assays, if used to screen CCP, could potentially be used to predict CCP with limited therapeutic potency. Importantly, in this study, PRT was not shown to drive antibody or activity positive CCP into this category. Moreover, the presence of samples with ratio >1 was viewed as reflecting the variability of the different assays (which were not formally quantified in this study, but have been examined elsewhere[22–26]) and was not attributed to an increase due to PRT.

In addition to immunoglobulins, other potential molecular mediators of CCP therapeutic activity including fibrinogen and VEGF, were preserved after PRT. Up to 69% of critically ill COVID-19 patients are coagulopathic leading to a pro-thrombotic state[45,46] and at autopsy, microvascular thrombosis have frequently been described.[47,48] Replacement of depleted fibrinogen at the same time as delivering neutralizing antibody may be important for reversing the coagulopathy and repairing endothelial cell damage. This may provide a potentially important therapeutic advantage for CCP over other passive immunotherapy strategies such as hyperimmune and recombinant antibody preparations. These data indicate that on average, a 200–400 ml dose of A/UVA-PRT CCP would contain approximately 600–1300 mg of fibrinogen providing potential to impact coagulopathy and endothelial cell health.

## 4.2 | Pathogen reduction treatment enables pooling of CCP

CP, as with all transfusable blood products, carries a risk of TTI from the newly emerged pathogen and other

unrecognized microbes, particularly in patients with impaired immune responses as described for severe COVID-19 patients.[49] Pathogen inactivation can effectively mitigate these risks. In addition, RNA viruses such as SARS-CoV-2 are prone to high mutation rates resulting in inter-patient and intra-patient epitope drift that can make a single clone of neutralizing antibody ineffective or susceptible to therapeutic resistance.[50,51] PRT reduces the increased risk of TTI associated with multi-donor pooling which can increase the diversity of the polyclonal neutralizing antibodies and provide more consistent levels of antibodies in CCP and reduce the risk of TRALI.

## 4.3 | PRT may reduce potentially deleterious factors associated with CSS

A growing body of data suggests that in SARS-CoV-2 infection, CSS is a major cause of ARDS, and other end-organ damage driving morbidity and mortality. CSS results from severe inflammation and an exaggerated immune response. While different cytokines have been implicated in CSS in viral infections, IL-1β, MCP-1, and MIP-1β have been regularly cited as key mediators. Increased levels of these cytokines have been hypothesized to be associated with and causative in initiating and promoting the COVID-19 inflammatory imbalance. Reduction of these cytokines, observed with A/UVA-PRT, may reduce the risk of inducing CSS in patients receiving CCP therapy. Use of this technology to reduce or remove pro-inflammatory cytokines associated with CSS in other disorders requiring transfusion of plasma products warrants further investigation.

## 4.4 | Potential for cross-reactive antibody with implications for future coronavirus epidemics

SARS-CoV-2 is closely related to β-coronaviruses SARS-CoV-1 (76% aa identity for spike, 90% aa identity for nucleocapsid protein) and MERS-CoV-1 (35% aa identity for spike, 48% aa identity for nucleocapsid protein).[38] This raises the possibility that CCP with immunoreactivity to SARS-CoV-2 may demonstrate cross-reactivity to the homologous proteins of SARS-CoV-1 or MERS-CoV-1. The COVAM microarray analysis detected reactivity with SARS-CoV-1 and MERS-CoV-1, indicative of cross-reactivity as the low prevalence and circumscribed geographic localization of these viruses makes it unlikely donors in this study were also exposed to either of these two viruses. Given the high homology between SARS-CoV-2 and SARS-CoV-1, it is surprising to see very little cross-reactivity observed with Spike protein. Also unexpectedly, 10% of all donors assayed in this study demonstrated cross-reactivity to MERS-CoV-1 despite lower amino acid identity than with SARS-CoV spike protein. These cross-reactive donors also have high neutralizing activity, raising the intriguing possibility that these CCP may also have neutralizing activity for MERS and other future corona aviruses with high levels of mortality.[52]

## CONFLICT OF INTEREST
AB, MVG, MG, and LMC are employees and shareholders of Cerus Corporation which markets the INTERCEPT Blood System. CTT, PVR, and DS are employees of ENable Biosciences which markets ADAP assay for SARS-CoV-2 detection. PLF is a shareholder in Antigen Discovery Inc. and Nano immune Inc. RRDA, GS, ZWM, MS, CDG, RM, OD, JR, DW, AZ, SK, and MPB have disclosed no conflicts of interest.

## ORCID
*Anil Bagri* https://orcid.org/0000-0001-9679-1211
*Zhen W. Mei* https://orcid.org/0000-0002-3810-2673
*Clara Di Germanio* https://orcid.org/0000-0002-6047-211X
*Orsolya Darst* https://orcid.org/0000-0003-3682-4338
*Dawn Ward* https://orcid.org/0000-0003-1672-740X
*Alyssa Ziman* https://orcid.org/0000-0002-1814-9319
*Laurence M. Corash* https://orcid.org/0000-0002-8615-9869

## REFERENCES
1. Yang W, Cao Q, Qin L, Wang X, Cheng Z, Pan A, et al. Clinical characteristics and imaging manifestations of the 2019 novel coronavirus disease (COVID-19): a multi-center study in Wenzhou city, Zhejiang, China. J Infect. 2020;80(4):388–93.
2. Guan WJ, Ni ZY, Hu Y, Liang WH, Ou CQ, He JX, et al. Clinical characteristics of coronavirus disease 2019 in China. N Engl J Med. 2020;382(18):1708–20.
3. Jean SS, Lee PI, Hsueh PR. Treatment options for COVID-19: the reality and challenges. J Microbiol Immunol Infect. 2020;53(3):436–43.
4. Bloch EM, Shoham S, Casadevall A, Sachais BS, Shaz B, Winters JL, et al. Deployment of convalescent plasma for the prevention and treatment of COVID-19. J Clin Invest. 2020;130(6):2757–65.
5. Enria DA, Briggiler AM, Sanchez Z. Treatment of argentine hemorrhagic fever. Antiviral Res. 2008;78(1):132–9.
6. Enria DA, Briggiler AM, Fernandez NJ, Levis SC, Maiztegui JI. Importance of dose of neutralising antibodies in treatment of argentine haemorrhagic fever with immune plasma. Lancet. 1984;2(8397):255–6.

7. Mair-Jenkins J, Saavedra-Campos M, Baillie JK, Cleary P, Khaw FM, Lim WS, et al. The effectiveness of convalescent plasma and hyperimmune immunoglobulin for the treatment of severe acute respiratory infections of viral etiology: a systematic review and exploratory meta-analysis. J Infect Dis. 2015; 211(1):80–90.

8. Soo YO, Cheng Y, Wong R, Hui DS, Lee CK, Tsang KK, et al. Retrospective comparison of convalescent plasma with continuing high-dose methylprednisolone treatment in SARS patients. Clin Microbiol Infect. 2004;10(7):676–8.

9. Lai ST. Treatment of severe acute respiratory syndrome. Eur J Clin Microbiol Infect Dis. 2005;24(9):583–91.

10. Cheng Y, Wong R, Soo YO, Wong WS, Lee CK, Ng MH, et al. Use of convalescent plasma therapy in SARS patients in Hong Kong. Eur J Clin Microbiol Infect Dis. 2005;24(1):44–6.

11. Salazar E, Christensen PA, Graviss EA, Nguyen DT, Castillo B, Chen J, et al. Treatment of coronavirus disease 2019 patients with convalescent plasma reveals a signal of significantly decreased mortality. Am J Pathol. 2020;190(11):2290–303.

12. Liu STH, Lin HM, Baine I, Wajnberg A, Gumprecht JP, Rahman F, et al. Convalescent plasma treatment of severe COVID-19: a propensity score-matched control study. Nat Med. 2020;26:1708–13.

13. Klassen SA, Senefeld JW, Johnson PW, Carter RE, Wiggins CC, Shoham S, et al. Evidence favoring the efficacy of convalescent plasma for COVID-19 therapy. medRxiv. 2020. doi:10.1101/2020.07.29.20162917.

14. Martinelli N, Montagnana M, Pizzolo F, Friso S, Salvagno GL, Forni GL, et al. A relative ADAMTS13 deficiency supports the presence of a secondary microangiopathy in COVID 19. Thromb Res. 2020;193:170–2.

15. Lo MW, Kemper C, Woodruff TM. COVID-19: complement, coagulation, and collateral damage. J Immunol. 2020;205(6): 1488–95.

16. Jhaveri KD, Meir LR, Flores Chang BS, Parikh R, Wanchoo R, Barilla-LaBarca ML, et al. Thrombotic microangiopathy in a patient with COVID-19. Kidney Int. 2020;98(2):509–12.

17. Gavriilaki E, Anyfanti P, Gavriilaki M, Lazaridis A, Douma S, Gkaliagkousi E. Endothelial dysfunction in COVID-19: lessons learned from coronaviruses. Curr Hypertens Rep. 2020;22(9):63.

18. Gavriilaki E, Brodsky RA. Severe COVID-19 infection and thrombotic microangiopathy: success does not come easily. Br J Haematol. 2020;189(6):e227–30.

19. Cure E, Cure MC. COVID-19 may predispose to thrombosis by affecting both vascular endothelium and platelets. Clin Appl Thromb Hemost. 2020;26:1076029620933945.

20. Prowse CV. Component pathogen inactivation: a critical review. Vox Sang. 2013;104(3):183–99.

21. Cascella M, Rajnik M, Cuomo A, Dulebohn SC, Di Napoli R. Features, evaluation, and treatment of coronavirus. Treasure Island, FL: StatPearls; 2020.

22. Tsai CT, Robinson PV, Spencer CA, Bertozzi CR. Ultrasensitive antibody detection by agglutination-PCR (ADAP). ACS Cent Sci. 2016;2(3):139–47.

23. Karp DG, Cuda D, Tandel D, Danh K, Robinson PV, Seftel D, et al. Sensitive and specific detection of SARS-CoV-2 antibodies using a high-throughput, fully automated liquid-handling robotic system. SLAS Technol. 2020;25(6):545–52.

24. Danh K, Karp DG, Robinson PV, Seftel D, Stone M, Simmons G, et al. Detection of SARS-CoV-2 neutralizing antibodies with a cell-free PCR assay. medRxiv. 2020. https://doi.org/10.1101/2020.05.28.20105692

25. Jasinskas A, Felgner J, Obiero JM, Norris PJ, Stone M, Simmons G, et al. Analysis of SARS-CoV-2 antibodies in COVID-19 convalescent plasma using a coronavirus antigen microarray. bioRxiv. 2020.

26. Ng DL, Goldgof GM, Shy BR, Levine AG, Balcerek J, Bapat SP, et al. SARS-CoV-2 seroprevalence and neutralizing activity in donor and patient blood. Nat Commun. 2020;11(1): 4698.

27. Hedde PN, Abram TJ, Jain A, Nakajima R, Ramiro de Assis R, Pearce T, et al. A modular microarray imaging system for highly specific COVID-19 antibody testing. Lab Chip. 2020; 20(18):3302–9.

28. Nie J, Li Q, Wu J, Zhao C, Hao H, Liu H, et al. Establishment and validation of a pseudovirus neutralization assay for SARS-CoV-2. Emerg Microbes Infect. 2020;9(1):680–6.

29. Jin J, Ma H, Xu L, An D, Sun S, Huang X, et al. Development of a Coxsackievirus A16 neutralization assay based on pseudoviruses for measurement of neutralizing antibody titer in human serum. J Virol Methods. 2013;187(2):362–7.

30. Hu J, Gao Q, He C, Huang A, Tang N, Wang K. Development of cell-based pseudovirus entry assay to identify potential viral entry inhibitors and neutralizing antibodies against SARS-CoV-2. Genes Dis. 2020;7:551–7.

31. Kozar RA, Peng Z, Zhang R, Holcomb JB, Pati S, Park P, et al. Plasma restoration of endothelial glycocalyx in a rodent model of hemorrhagic shock. Anesth Analg. 2011;112(6):1289–95.

32. Tang Y, Liu J, Zhang D, Xu Z, Ji J, Wen C. Cytokine storm in COVID-19: the current evidence and treatment strategies. Front Immunol. 2020;11:1708.

33. Song P, Li W, Xie J, Hou Y, You C. Cytokine storm induced by SARS-CoV-2. Clin Chim Acta. 2020;509:280–7.

34. Cao X. COVID-19: immunopathology and its implications for therapy. Nat Rev Immunol. 2020;20(5):269–70.

35. Italiani P, Puxeddu I, Napoletano S, Scala E, Melillo D, Manocchio S, et al. Circulating levels of IL-1 family cytokines and receptors in Alzheimer's disease: new markers of disease progression? J Neuroinflammation. 2018;15(1):342.

36. Valkovic T, Babarovic E, Lucin K, Štifter S, Aralica M, Seili-Bekafigo I, et al. Plasma levels of monocyte chemotactic protein-1 are associated with clinical features and angiogenesis in patients with multiple myeloma. Biomed Res Int. 2016;2016: 7870590.

37. van Breemen MJ, de Fost M, Voerman JS, Laman JD, Boot RG, Maas M, et al. Increased plasma macrophage inflammatory protein (MIP)-1alpha and MIP-1beta levels in type 1 Gaucher disease. Biochim Biophys Acta. 2007;1772(7):788–96.

38. Grifoni A, Sidney J, Zhang Y, Scheuermann RH, Peters B, Sette A. A sequence homology and bioinformatic approach can predict candidate targets for immune responses to SARS-CoV-2. Cell Host Microbe. 2020;27(4):671–680 e672.

39. Klein SL, Pekosz A, Park HS, Ursin RL, Shapiro JR, Benner SE, et al. Sex, age, and hospitalization drive antibody responses in a COVID-19 convalescent plasma donor population. J Clin Invest. 2020;130:6141–50.

40. DomBourian MG, Annen K, Huey L, Andersen G, Merkel PA, Jung S, et al. Analysis of COVID-19 convalescent plasma for SARS-CoV-2 IgG using two commercial immunoassays. J Immunol Methods. 2020;486:112837.

41. Benner SE, Patel EU, Laeyendecker O, Pekosz A, Littlefield K, Eby Y, et al. SARS-CoV-2 antibody avidity responses in COVID-19 patients and convalescent plasma donors. J Infect Dis. 2020;222:1974–84.

42. Dean CL, Hooper JW, Dye JM, Zak SE, Koepsell SA, Corash L, et al. Characterization of Ebola convalescent plasma donor immune response and psoralen treated plasma in the United States. Transfusion. 2020;60:1024–31.

43. Pierson TC, Diamond MS. The continued threat of emerging flaviviruses. Nat Microbiol. 2020;5(6):796–812.

44. Lanteri MC, Santa-Maria F, Laughhunn A, Girard YA, Picard-Maureau M, Payrat JM, et al. Inactivation of a broad spectrum of viruses and parasites by photochemical treatment of plasma and platelets using amotosalen and ultraviolet A light. Transfusion. 2020;60(6):1319–31.

45. Llitjos JF, Leclerc M, Chochois C, Monsallier JM, Ramakers M, Auvray M, et al. High incidence of venous thromboembolic events in anticoagulated severe COVID-19 patients. J Thromb Haemost. 2020;18(7):1743–6.

46. Klok FA, Kruip M, van der Meer NJM, Arbous MS, Gommers DA, Kant KM, et al. Confirmation of the high cumulative incidence of thrombotic complications in critically ill ICU patients with COVID-19: an updated analysis. Thromb Res. 2020;191:148–50.

47. Carsana L, Sonzogni A, Nasr A, Rossi RS, Pellegrinelli A, Zerbi P, et al. Pulmonary post-mortem findings in a series of COVID-19 cases from northern Italy: a two-centre descriptive study. Lancet Infect Dis. 2020;20(10):1135–40.

48. Ackermann M, Verleden SE, Kuehnel M, Haverich A, Welte T, Laenger F, et al. Pulmonary vascular endothelialitis, thrombosis, and angiogenesis in Covid-19. N Engl J Med. 2020;383(2):120–8.

49. Mazzoni A, Salvati L, Maggi L, Capone M, Vanni A, Spinicci M, et al. Impaired immune cell cytotoxicity in severe COVID-19 is IL-6 dependent. J Clin Invest. 2020;130(9):4694–703.

50. Wang C, Liu Z, Chen Z, Huang X, Xu M, He T, et al. The establishment of reference sequence for SARS-CoV-2 and variation analysis. J Med Virol. 2020;92(6):667–74.

51. Benvenuto D, Giovanetti M, Salemi M, Prosperi M, de Flora C, Junior Alcantara LC, et al. The global spread of 2019-nCoV: a molecular evolutionary analysis. Pathog Glob Health. 2020;114(2):64–7.

52. Pormohammad A, Ghorbani S, Khatami A, Farzi R, Baradaran B, Turner DL, et al. Comparison of confirmed COVID-19 with SARS and MERS cases - clinical characteristics, laboratory findings, radiographic signs and outcomes: a systematic review and meta-analysis. Rev Med Virol. 2020;30(4):e2112.

## SUPPORTING INFORMATION

Additional supporting information may be found in the online version of the article at the publisher's website.

**How to cite this article:** Bagri A, de Assis RR, Tsai C-T, Simmons G, Mei ZW, Von Goetz M, et al. Antibody profiles in COVID-19 convalescent plasma prepared with amotosalen/UVA pathogen reduction treatment. Transfusion. 2022;62:570–83. https://doi.org/10.1111/trf.16819